ELSEVIER

Catalysis Today 81 (2003) 227–245

CATALYSIS TODAY

www.elsevier.com/locate/cattod

Efficient oxyfunctionalization of *n*-hexane by aqueous H_2O_2 over a new TS-PQ^{TM} catalyst

Istvan Halasz*, Mukesh Agarwal, Eric Senderov, Bonnie Marcus

PQ Corporation, R&D Center, 280 Cedar Grove Road, Conshohocken, PA 19428, USA

Abstract

The oxyfunctionalization of *n*-hexane by aqueous H_2O_2 was found to proceed substantially faster over a titanium-containing pentasil type catalyst denoted as TS-PQ^{TM} (a trademark of PQ corporation for this titanium silicate material), than over other comparable titanium-containing zeolites. This catalyst has an unprecedented >99% efficiency in utilizing H_2O_2 in the oxidation of a paraffin. The effect of temperature, stirring rate, pH, solvent, and reactant ratios on the reaction rate, H_2O_2 efficiency, and product selectivity were evaluated over the TS-PQ^{TM} silicate using a statistically designed catalytic test performed in an atmospheric batch reactor. Accurate reaction times were determined by continuously monitoring H_2O_2 consumption. Hydrated and in situ dehydrated TS-PQ^{TM} titanium silicate samples were studied in a diffuse reflectance (DRIFT) cell by FT-UV and FT-IR spectroscopy. Unlike TS-1 catalysts that mainly contain isolated Ti^{4+} ions in tetrahedral lattice positions, TS-PQ^{TM} silicate contains tetrahedral and higher coordination Ti^{4+} ions. Slightly acidic conditions affect favorably the reaction rate and C_2 regioselectivity over the TS-PQ^{TM} catalyst. In contrast to TS-1, applying methanol (MOH) as co-solvent had little or negative effect on the reaction rate and the selectivity of TS-PQ^{TM} catalyst for the oxyfunctionalization of *n*-hexane.

Keywords: Selective oxidation; Oxyfunctionalization; Paraffin; Hydrocarbon; *n*-Hexane; Catalytic; Microporous; TS-1; Titanium silicate

1. Introduction

The degree of difficulty in inserting only one oxygen to form alcohols and oxo-compounds in a straight chain, saturated hydrocarbon or paraffin is well known. The problem is that initiating the reaction requires such harsh conditions, it does not want to stop but wants to go on to multi-oxygenation or full combustion. TS-1 was the first effective heterogeneous catalyst that could initiate selective oxidation on paraffins with dilute aqueous H_2O_2 at temperatures below 100 °C [1,2]. This microporous MFI type titanium silicate is the parent compound of a constantly growing family of micro- and mesoporous titanium silicate catalysts [3–8]. During the past decade or so, considerable research work was devoted to exploring the structure of TS-1 and its effect on the conversion and product distribution in the oxidation of various paraffins [1–5,9–34]. However, this process is still not well understood.

A typical TS-1 catalyst contains mainly isomorphously substituted tetrahedral Ti atoms in an MFI type silicate framework [3,10,35,36]. However, an increasing number of studies indicate that in some catalytically active samples the TS-1 crystal lattice might be distorted by non-isomorphously substituted titanium ions and other structural defects [28,34,37–45]. Recently we compared the catalytic activity and selectivity of an isomorphously substituted TS-1 zeolite with those of some distorted structures in the oxyfunctionalization of *n*-hexane by aqueous H_2O_2 at near

* Corresponding author.
E-mail address: istvan.halasz@pqcorp.com (I. Halasz).

0920-5861/03/$ – see front matter © 2003 Elsevier Science B.V. All rights reserved.
doi:10.1016/S0920-5861(03)00122-6

ambient reaction conditions [34]. One catalyst that contained virtually no isolated tetrahedral Ti^{4+} ions in lattice positions, denoted here as TS-PQ^{TM} titanium silicate, was found to be more active and selective for this process than other heterogeneous catalysts reported thus far. The TS-PQ^{TM} silicate retained these excellent catalytic properties even in the absence of any homogenizing solvent. *n*-Hexane is reportedly the most reactive paraffin over TS-1 [1,2,9,10] when a non-reactive co-solvent, usually methanol (MOH) or acetone, is added to the non-miscible hydrocarbon and aqueous phases.

It is believed that these co-solvents can affect the catalytic process in various ways: (i) they might help to prevent formation of polymers from secondary oxidation products [23]; (ii) they might facilitate the penetration of hydrophobic micropores for the aqueous phase [27]; (iii) they might form a homogeneous phase by partitioning the non-polar (*n*-hexane) and polar (H_2O_2) molecules [32] and (iv) they might generate and stabilize Ti^{4+} related lattice defects as catalytically active sites [33,46]. In this paper, we systematically check the co-solvent effect along with the effect of other fundamental reaction parameters on the catalytic activity and selectivity of TS-PQ^{TM} silicate in the oxyfunctionalization of *n*-hexane by aqueous H_2O_2. We did this using a statistically designed set of experiments.

2. Experimental

2.1. Catalysts and materials

Pure *n*-hexane (98%), methanol (99.98%), hexanol and hexanone isomers (>98%), and 30% aqueous H_2O_2 from Fluka and Sigma–Aldrich were used for catalytic tests and GC analysis. The accurate concentration of H_2O_2 was periodically determined by permanganometric titration.

The TS-PQ^{TM} titanium silicate was made according to a pending patent description [47] and used in powder form for catalytic measurements. The average particle size of this MFI type crystalline material was 0.1–0.3 μm based on Hitachi 3500N SEM measurements. The nominal Si/Ti ratio was ∼55. According to laser Raman quantification [34], the calcined product contained ∼200 ppm Anatase (TiO_2).

2.2. Catalytic measurements and product analysis

Details of our atmospheric catalytic system have been described elsewhere [34]. Briefly, a 100 ml volume glass reactor equipped with a water-cooled reflux, a stirrer, and a Type JJ9 Cole Palmer redox (ORP) electrode was heated externally by an electromantle controlled by a Staco Series 500 temperature controller and a thin (1/64 in.) type T thermocouple placed inside the reactor below the liquid level. A variable speed magnetic stirrer was used for experiments with <1000 rpm, and a PolyScience Model X-120 homogenizer for stirring rates from 5000 to 30,000 rpm. A Masterflex liquid pump dosed the necessary amount of 30% aqueous H_2O_2 into the reactor from a Teflon container placed onto an Ohaus Precision Standard balance. The ORP controller started and stopped the liquid pump automatically to maintain ∼0.1 mol H_2O_2/l concentration in the reactor. The weight change of the H_2O_2 container was registered every 20 s during the catalytic process, and end of the reaction was designated to be when the signal from the balance did not change for 10 min or more.

For the catalytic test, a desired amount of catalyst powder was weighed into the reactor first and saturated with 0.6 ml aqueous 30% H_2O_2 solution per gram zeolite (∼200 mmol H_2O_2/mmol Ti^{4+}). After adding the necessary amount of *n*-hexane, the stirrer was started and the heater was set. Table 1 contains details of the reaction conditions used and a description is given in the Section 3 of this paper.

After reaction, the liquid phases were homogenized with methanol and analyzed using an HP-6890 type GC–MS using a 30 m/250 μm HP-19091N-133 capillary column and temperature programming between 35 and 120 °C.

Blank experiments without catalyst at 50 °C indicated immeasurably low H_2O_2 consumption during a period of 120 min which is substantially longer than the longest oxidation time at our reaction conditions (∼60 min). Therefore, we believe that spontaneous H_2O_2 decomposition or homogeneous hydrocarbon oxidation does not occur at these conditions. The utilization of H_2O_2 for hexane oxidation versus decomposition was calculated from the material balance of reacted *n*-hexane and H_2O_2 molecules according to the following stoichiometry.

Table 1
Designed variation of experimental conditions for the oxidation of *n*-hexane by 30% aqueous H_2O_2; L_{18} ($2^1 \times 3^7$) mixed level orthogonal array [48]

Experiment #	Temperature, T (°C)	Catalyst loading (HTi) (mol *n*-hexane/mmol Ti)	MetOH/*n*-hexane ratio (MOH) (ml/ml)	pH	Stirring rate (rpm)	H_2O_2 pumping rate, V (ml/min)
1	40	1.28	0.0	4	500	0.5
2	40	0.64	0.5	9	5000	1.0
3	40	0.10	1.0	7	10000	2.0
4	50	1.28	0.5	7	5000	2.0
5	50	0.64	1.0	4	10000	0.5
6	50	0.10	0.0	9	500	1.0
7	60	1.28	1.0	9	5000	0.5
8	60	0.64	0.0	7	10000	1.0
9	60	0.10	0.5	4	500	2.0
10	40	1.28	1.0	7	500	1.0
11	40	0.64	0.0	4	5000	2.0
12	40	0.10	0.5	9	10000	0.5
13	50	1.28	0.0	9	10000	2.0
14	50	0.64	0.5	7	500	0.5
15	50	0.10	1.0	4	5000	1.0
16	60	1.28	0.5	4	10000	1.0
17	60	0.64	1.0	9	500	2.0
18	60	0.10	0.0	7	5000	0.5

$$CH_3–CH_2–CH_2–CH_2–CH_2–CH_3 + H_2O_2 \rightarrow CH_3–CHOH–CH_2–CH_2–CH_2–CH_3 + H_2O$$

$$CH_3–CHOH–CH_2–CH_2–CH_2–CH_3 + H_2O_2 \rightarrow CH_3–CO–CH_2–CH_2–CH_2–CH_3 + 2H_2O$$

2.3. Spectroscopy

A Nicolet Magna 550 FTIR, Kaiser Optical Systems HoloProbe laser Raman, and a Bruker IFS66/S spectrometer with variable Fourier transform capability from the far IR (~100 cm^{-1}) to the deep UV (~190 nm) range were used for measuring various properties of TS-PQ™ silicate.

Raman measurements were made at atmospheric conditions in a homemade sample holder providing ~90 mW laser power on the sample. The sample container was attached to a Mark II type probe connected via fiber optics to a 200 mW Nd:YAG diode pumped laser (frequency doubled to 532 nm) and a charge coupled device (CCD) detector.

All other spectroscopic measurements were carried out either at atmospheric conditions using a single bounce diamond attenuated total reflectance (ATR) accessory from ASI Applied Systems or in ~10^{-3} Pa vacuum using a diffuse reflectance (DRIFT) cell from Harrick Scientific. The DRIFT cell is equipped with CaF_2 windows and can be heated externally up to 600 °C which corresponds to ~400 °C measured directly in the sample. By switching beam splitters and detectors, the in situ calcined and evacuated samples could be characterized in the full range from 900 to 52,000 cm^{-1}. All DRIFT measurements were made after cooling the sample to room temperature using either a CaF_2 or a Teflon background and results were converted to Kubelka-Munk units. Liquid nitrogen cooled MCT, InSb, and D-530/2 type PMT (photo multiplier tube) detectors were used for measurements in the MIR, NIR, and UV ranges, respectively. Further details of our spectroscopic equipment and methods are described elsewhere [34].

2.4. Statistical experiment design and data analysis

The JMP software from SAS Institute [48] was used to design a representative set of experiments to evaluate the effects of various reaction parameters on the rate of reaction and the distribution of products. Data analysis was performed using the interactive statistics

and graphics capabilities of this program. This paper presents the Pareto plot based screening of reaction parameter effects. The Pareto plots let us visualize the orthogonally normalized, scaled estimates of the impact of variables on the conversion, selectivity, and other characteristics of the process.

3. Results

3.1. Design of catalytic experiments

The reaction conditions published for the selective oxyfunctionalization of *n*-hexane with H_2O_2 over TS-1 vary widely. Typically, results are reported on batch experiments carried out using a specific set of reaction variables chosen by the investigator. In those papers that give the necessary information to calculate the nominal Si/Ti ratio of zeolite, it varies between about 30 and 90; the reaction temperature varies from 50 to 100 °C, the contact time from 1 to 24 h, the reactant ratio from 0.5 to 3.5 (mol *n*-hexane/mol H_2O_2), the catalyst loading (from 0.04 to 1.5 mol *n*-hexane/g TS-1), and the solvent content from 0 to around 11 (ml methanol or acetone/ml *n*-hexane) [34].

To design a finite, statistical set of experiments for TS-PQ^{TM} catalyst, we considered these experimentally probed parameter ranges for setting minima and maxima of reaction variables. We found a total of seven variables that might fundamentally affect the reaction outcome at our experimental arrangement. One of them, the effect of stabilizer additive in H_2O_2, gave only two choices (present or not) while the others were calculated with three values near the minimum, middle, and maximum of their ranges. Thus, the L_{18} ($2^1 \times 3^7$) type mixed level orthogonal array [48] was selected as an experimental design that permits statistically significant correlations with results from 18 experiments. Table 1 shows that in the ultimate reaction parameter arrangement, we kept only the 6 three level variables and did not run experiments with non-stabilized H_2O_2 solution.

To probe the effect of temperature, 40, 50, and 60 °C were selected because we have never observed conversion below 40 °C [34] and our atmospheric reactor did not allow experiments above 60 °C. (H_2O and hexane can form azeotropic mixture with a boiling point of 61.6 °C [49]). The amounts of *n*-hexane and catalyst were adjusted according to the limiting 100 cm^3 reactor volume to cover the common catalyst loading range. We used only methanol as co-solvent with ≤ 1 (ml MetOH/ml *n*-hexane) ratio because we deemed the addition of more co-solvent impractical. It is well known that H_2O_2 can oxidize both at acidic and basic conditions [50]. Thus, the pH of the H_2O_2 solution was adjusted with either HNO_3 or NH_4OH to 4, 7, and 9 before pumping it into the reactor. The last two columns of Table 1 show the selected stirring rates and H_2O_2 pumping speeds that were specific parameters for our reactor setting.

We wish to emphasize that these experiments are intended to screen the impact of various reaction variables on the outcome of this reaction and cannot substitute the detailed kinetic study of this process. In lack of necessary information, material transport has not been separated from surface processes such as sorption and chemical transformation, hence data are not applicable to calculate the apparent activation energy or rate constants for various reaction steps. Likewise, the comparison of catalyst activity with published data is only valid for the overall process that involves the rates of both material transport and surface reaction.

3.2. Catalytic results and catalyst properties

Table 2 summarizes the results of catalytic experiments. Note that two, Experiments 6 and 18, were not done. The first and second columns show the amount of *n*-hexane before reaction and the total amount of H_2O_2 added to the reactor. The third column shows the titanium sites in the sample which is needed to calculate the reaction rates assuming that each Ti^{4+} ion is part of an active center ensemble. The composition of the organic phase after reaction is shown in the last five columns. Neither primary oxygenated products nor dual oxygenates were found in measurable amounts. With our experimental setup, the reaction time in column # 4 was also a dependent variable.

We found that reactions stopped before reaching total hydrocarbon conversion despite ample H_2O_2 supply. Fig. 1 shows a few examples for typical catalytic runs. The initial H_2O_2 consumption can be either steep (Test # 9) or flat (Test # 15) followed by either monotonously (Tests # 5 and # 11) or stepped (Tests # 9 and # 15) H_2O_2 consumption until a steady state condition is reached, i.e. no more oxidation

Table 2
Results of catalytic experiments at conditions according to Table 1

Experiment #	Reactants		Ti concentration (μmol)	Time of reaction (s)	Products from GC analysis				
	n-Hexane (mmol)	H_2O_2 (mmol)			*n*-Hexane (mmol)	2-ol (mmol)	3-ol (mmol)	2-on (mmol)	3-on (mmol)
1	297.8	7.04	232.3	179	290.8	0.50	0.00	2.23	3.77
2	148.9	0.00	232.3	0	148.9	0.00	0.00	0.00	0.00
3	101.5	4.10	1515.4	3590	97.9	0.00	0.00	0.50	3.06
4	148.9	0.00	116.0	0	148.9	0.00	0.00	0.00	0.00
5	190.0	62.12	232.1	879	127.9	3.75	0.56	25.07	28.16
6	300.0	0.00	3030.8	na	na	na	na	na	na
7	148.9	0.00	116.0	0	148.9	0.00	0.00	0.00	0.00
8	297.8	6.80	466.2	3610	291.1	1.31	0.00	0.50	3.61
9	190.0	115.07	1515.4	1676	116.7	18.40	7.88	2.57	18.18
10	148.9	0.00	116.0	0	148.9	0.00	0.00	0.00	0.00
11	297.8	12.55	466.2	559	278.3	1.42	0.00	2.34	14.23
12	148.9	0.00	1515.4	0	148.9	0.00	0.00	0.00	0.00
13	297.8	0.00	232.1	0	297.8	0.00	0.00	0.00	0.00
14	148.9	0.00	232.1	0	148.9	0.00	0.00	0.00	0.00
15	148.9	55.58	1515.4	3892	144.1	1.04	0.00	0.20	2.52
16	148.9	46.89	116.0	1337	144.3	1.04	0.00	0.00	2.52
17	148.9	0.00	232.1	0	148.9	0.00	0.00	0.00	0.00
18	300.0	0.00	3030.8	na	na	na	na	na	na

takes place. The reasons for the delayed steps or the total reaction stops are not clear. It is possible that confined oxidation products gradually block access to the active sites [1]. As Table 2 indicates, the reaction time from the beginning of H_2O_2 consumption until it stops can vary from a few minutes to about 1 h. This time variation might depend on the rate of both transport and surface processes.

In the 16 experiments presented, the turnover rates (TOR) varied from TOR = 0.04 (Experiment # 3;

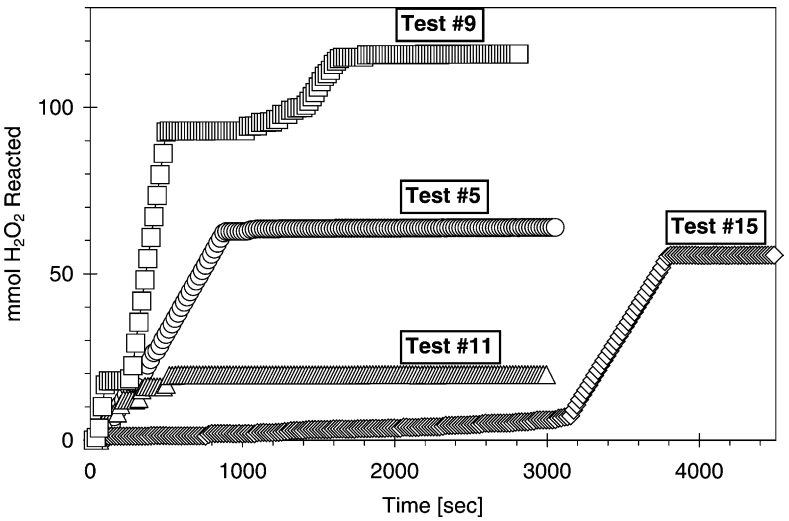

Fig. 1. Oxidation of *n*-hexane by 30% aqueous H_2O_2 at the test conditions 5, 9, 11, and 15 in Table 1.

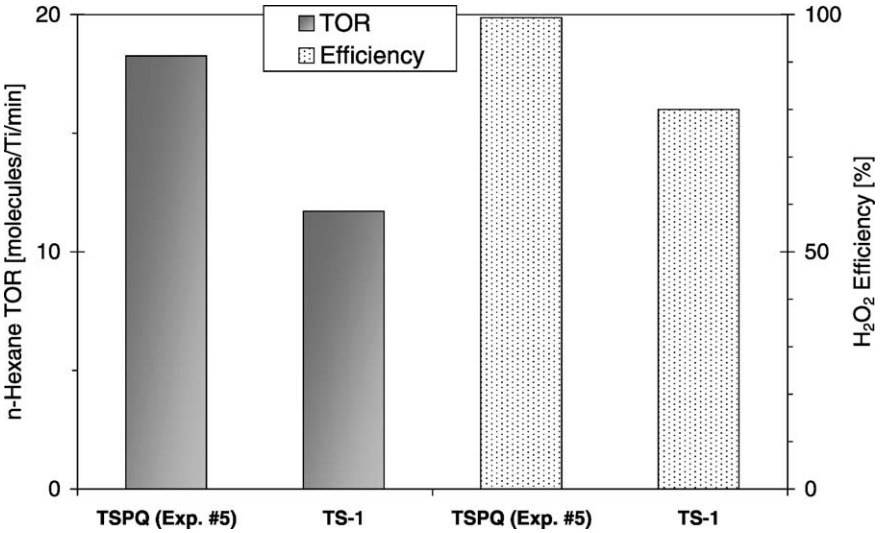

Fig. 2. Comparison of the turnover rates (TOR) and H_2O_2 efficiencies of the TS-PQ^{TM} catalyst and the most active TS-1 catalyst found in the literature [9]. Reaction conditions for TS-PQ^{TM} catalyst are given in Table 1, Experiment # 5. For TS-1 (Si/Ti ∼63) the reaction temperature was 100 °C, catalyst-loading 1.2 (mol *n*-hexane/mol Ti), solvent rate 3 ml acetone/ml *n*-hexane and the reaction time 3600 s.

not counting zero conversions) to TOR = 18.3 (mmol *n*-hexane/mmol Ti/min) (Experiment # 5). The maximum value is lower than our previously reported best TOR [34], but still substantially higher than the best data we could find in the literature (Fig. 2). In addition, the selectivity of TS-PQ^{TM} silicate for utilizing H_2O_2 was also excellent as is seen at the conditions of Experiment # 5. It is not clear at this time how important are the transport processes in attaining such outstanding reaction rates and efficiencies over the TS-PQ^{TM} silicate compared to those over TS-1.

The high-resolution FT-UV spectra in Fig. 3 demonstrate that, unlike a typical TS-1 that contains mainly isomorphously substituted, isolated, tetrahedral Ti^{4+} ions with an adsorption maximum at <210 nm [4,34,36,51–56], TS-PQ has substantial UV

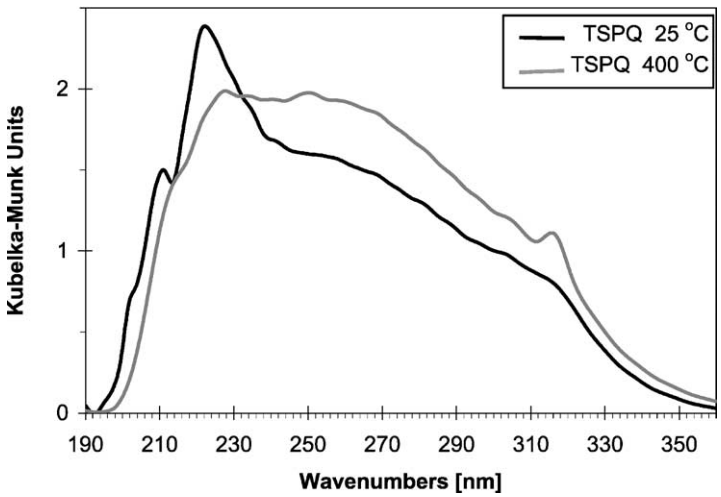

Fig. 3. FT-UV–DRIFT spectra of TS-PQ^{TM} silicate after evacuation at 3×10^{-3} Pa at 25 and 400 °C. Resolution 0.5 nm.

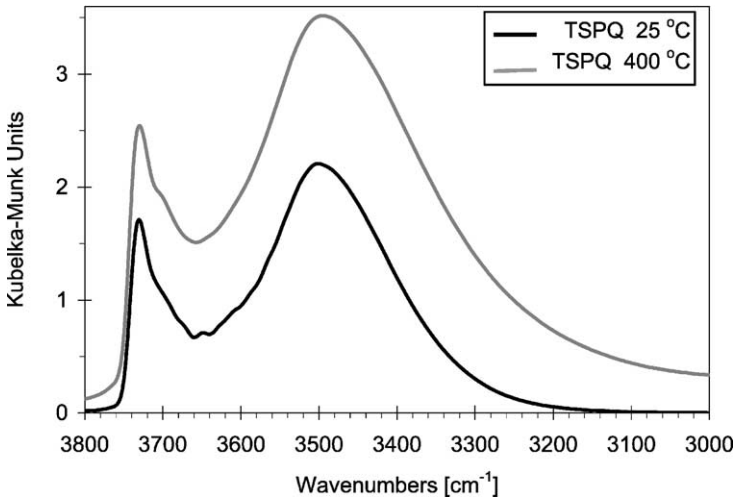

Fig. 4. FTIR–DRIFT spectra of TS-PQ^{TM} silicate at the same conditions as in Fig. 3.

absorption only above 220 nm especially when dehydrated at 400 °C. The adsorption near 220 nm is probably associated with non-isolated tetrahedral Ti^{4+} ions that appear sometime in the spectra of certain amorphous $SiTiO_x$ gels [57–60] and that have also been observed in acid treated Ti-MWW [61]. Adsorption above approximately 300 nm is typical for crystalline TiO_2 while the adsorption bands from 230 to 290 nm are likely due to variously coordinated octahedral Ti^{4+} ions [54–60]. The effect of high temperature dehydration on the coordination conditions of Ti^{4+} ions in TS-PQ^{TM} silicate is exactly the opposite of those reported over some defect-free isomorphously substituted TS-1 zeolites which show an increase in the adsorption band at ∼208 nm upon dehydration [3].

The FTIR spectra in Figs. 4 and 5 were measured at exactly the same conditions as those in Fig. 3. The 3730 cm^{-1} band represents the well-known

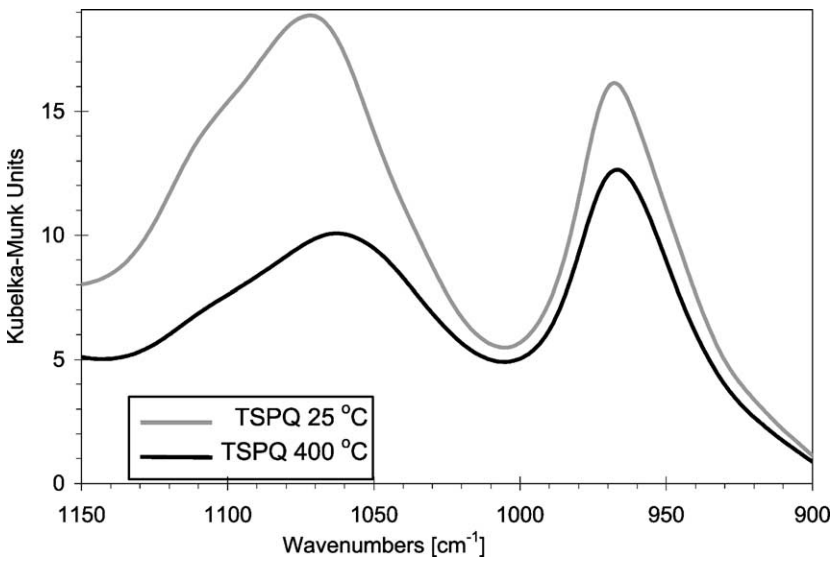

Fig. 5. FTIR–DRIFT spectra of TS-PQ^{TM} silicate at the same conditions as in Fig. 3.

fundamental stretching vibration of isolated terminal Si–OH groups and the broad band with about 3500 cm^{-1} maximum is typical for an array of hydrogen bonded hydroxyl groups [16,34,44,56,62]. Fig. 4 indicates that the overall intensity of hydroxyl vibrations decreases with increasing calcination temperature, but the ratio of isolated and hydrogen bonded hydroxyls remains largely intact after dehydration at higher temperature. It was shown previously [34] that this material contains some molecular water that evaporates during evacuation at high temperature. Thus, the decrease of the overall hydroxyl intensity likely reflects this water removal.

Conceivably this dehydration causes the observed changes in the FT-UV spectra of calcined TS-PQ^{TM} titanium silicate (Fig. 3) presumably by changing the charge transfer conditions of titanium ions when the water molecules are leaving their coordination sphere. Fig. 5 shows that the well-known [34,45,46,52,63] 960 cm^{-1} vibration associated with Ti–O–Si bonds is present in the FTIR spectra of both the room temperature and the 400 °C evacuated samples. Therefore, the titanium atoms of TS-PQ^{TM} silicate appear to remain primarily chemically bound to the MFI structured silicate lattice after the high temperature treatment.

3.3. Screening reaction variable effects

The effect of the reaction parameters outlined in Table 1 on the rate and selectivity of *n*-hexane oxidation over the TS-PQ^{TM} catalyst were evaluated by building a statistical model with minimum 0.25 significance probability using stepwise regression and visualized with the help of Pareto plots [48]. Only those correlations that gave $r^2 > 0.9$ correlation coefficients were taken into account.

Since different amounts of catalyst were used for the experiments, comparing the overall hydrocarbon conversions is meaningless. Instead, we compared the turnover numbers (TON) of *n*-hexane, which gives the hydrocarbon conversion per unit catalyst and permits comparisons with other catalysts having different Si/Ti ratios. Fig. 6 shows that mainly the pH and, to a lesser extent the stirring rate (rpm), determine how many hexane molecules are converted over each Ti atom before the reaction stops. The mutual effect of these variables together with that of the pumping rate

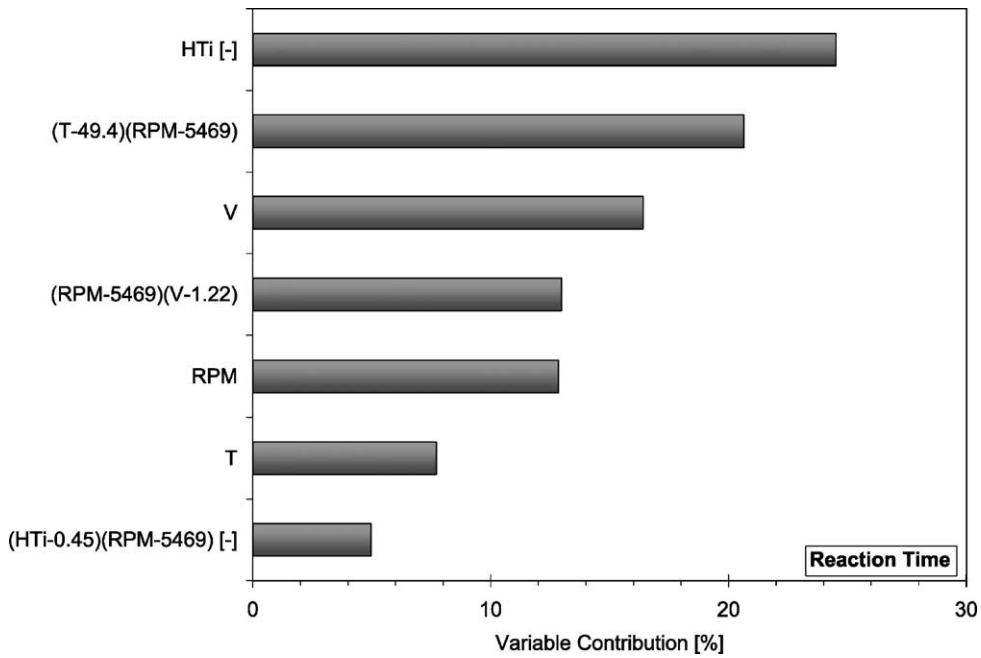

Fig. 6. Effect of reaction variables on the duration of reaction in the oxyfunctionalization of *n*-hexane by 30% aqueous H_2O_2; Pareto plot.

of H_2O_2 (V) and temperature (T) are also important, but these latter variables have clearly much smaller individual impact on the *n*-hexane TON than pH or rpm. For brevity we use the short symbols of variables as given in Table 1. The negative sign in brackets behind the symbols and expressions in the Pareto plots are indicative of the fact that those parameters have a negative impact on TON (and other parameters shown in the next Pareto plots) while they have a positive impact when this negative sign is missing. Thus, Fig. 6 indicates for example that increasing pH (higher basicity) or H_2O_2 pumping rate cause a decrease in TON while increased stirring rates increase TON. This latter result suggests that the transport of molecules to and/or from the particles affects how many molecules are able to react before the active sites become inactive or inaccessible.

Fig. 7 indicates that the duration of reaction time decreases when the catalyst loading (HTi) increases, presumably due to an increased concentration gradient between the external liquid phase and the micropores of the catalyst in which confined molecules prefer an oriented arrangement [64] that can hinder transport processes. The combined effect of temperature and stirring rate is also strong. The effect of the H_2O_2 pumping speed suggests that the active sites of TS-PQ^{TM} catalyst remain accessible longer when ample H_2O_2 is present. The need for more H_2O_2 might also be associated with the acidity that the H_2O_2 imparts.

Fig. 8 shows the TOR of *n*-hexane. The TOR is a measure of the rate at which the individual hydrocarbon molecules react on an active site and mainly depends on the pH. While TON, the average number of *n*-hexane molecules that can convert on an active site assuming that each titanium atom participates in one active site ensemble, varies from about 2.4 (Experiment # 3 in Table 2) to about 48.4 (mol *n*-hexane/mol Ti) (Experiment # 9 in Table 2), the TOR varies from 0.04 (Experiment # 3 in Table 2) to 18.3 (mol *n*-hexane/mol Ti/min) (Experiment # 5 in Table 2). Thus, the virtual residence time of a hexane molecule on a Ti-related active center can vary from about 3.3 s. (Experiment # 5 in Table 2) to 1528 s. (Experiment # 3 in Table 2). Since the catalytic conversion of a molecule usually happens within the range of 10^{-3}–10^{2} s [50,65,66], the much longer virtual residence time in this system suggests that either an

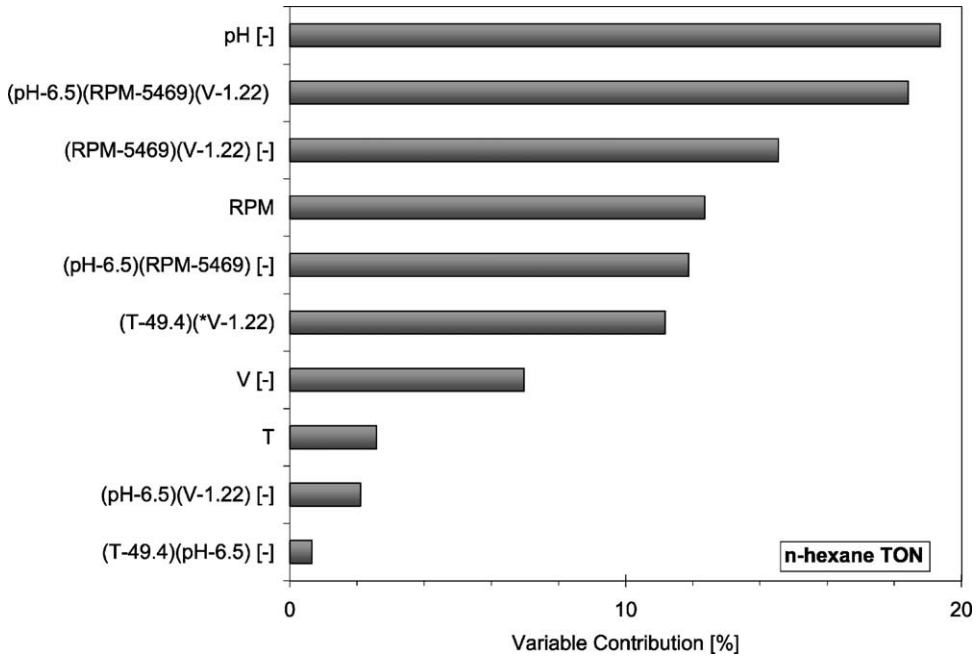

Fig. 7. Effect of reaction variables on the turnover number (TON) of *n*-hexane molecules per titanium atoms in the reactor; Pareto plot.

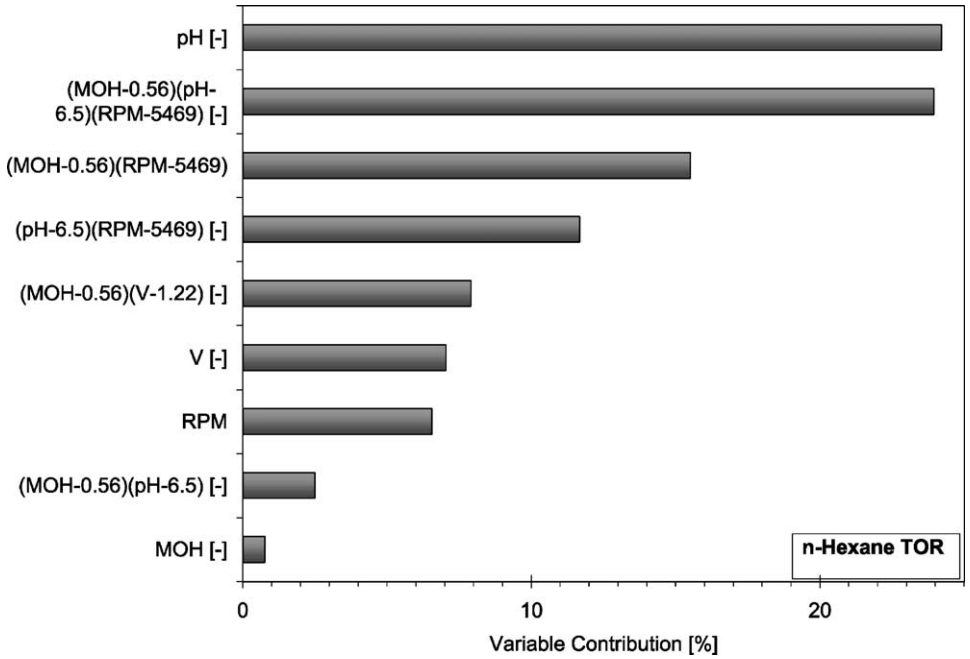

Fig. 8. Effect of reaction variables on the turnover rate (TOR) of *n*-hexane molecules measured in (mol *n*-hexane/mol Ti/min) units; Pareto plot.

extremely slow diffusion occurs or a significant part of the titanium atoms do not participate in any active site ensemble. Fig. 8 indicates that the temperature and stirring rate only slightly affect the TOR of *n*-hexane. Since diffusion depends on these reaction variables, it has presumably low impact on the TOR of *n*-hexane. Consequently the titanium content of TS-PQ^{TM} silicate must be only partially accessible as active site for the reactant molecules.

According to Figs. 6 and 8, the effect of methanol (MOH) is negligible on both the TON and TOR of *n*-hexane. Therefore, one cannot expect substantial rate improvement in the oxyfunctionalization process over TS-PQ^{TM} catalyst in the presence of methanol co-solvent. Note that this reaction also proceeds over isomorphously substituted, defect-free TS-1 catalysts in the absence of any co-solvent but methanol improves the reaction rate over such catalysts [10].

Figs. 9 and 10 indicate that both the TON and TOR of H_2O_2 largely depend on the same reaction variables as those of *n*-hexane (Figs. 6 and 8). The positive effect of acidity accounts for about 30% of the effect of all reaction variables that have an impact on the reaction. It has been noted that in the same reaction with TS-1 catalysts, the rate of H_2O_2 consumption increases in the presence of HCl while addition of HF is detrimental [10].

There are several selectivity aspects that can be considered for the oxyfunctionalization of paraffins. For instance, an important issue is the efficiency of using H_2O_2 for hydrocarbon oxidation without spontaneous decomposition of this relatively expensive oxidant. Fig. 2 shows an example for >99% H_2O_2 utilization over TS-PQ^{TM} silicate in Experiment # 5. Experiments # 1 and # 11 from Table 2 are another two examples. Some other results in Table 2 show much lower efficiencies (8% in Experiment # 15), but we were unable to find any statistically significant correlation between these numbers and the reaction variables tested. This observation implies that the efficient use of H_2O_2 is largely an intrinsic property of the TS-PQ^{TM} silicate related to its specific structure.

Another selectivity aspect is the production of 2-hexanol, 3-hexanol, 2-hexanone, or 3-hexanone. Lower pH and increased stirring rate improve the selectively for the first two oxygenates yet the combined

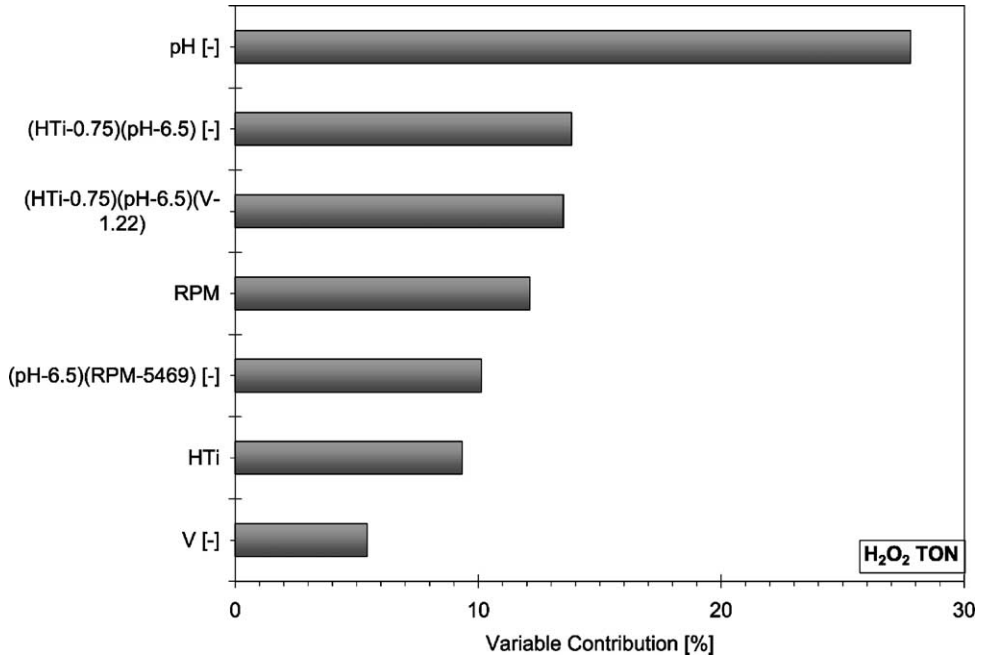

Fig. 9. Effect of reaction variables on the turnover number (TON) of H_2O_2 molecules per titanium atoms in the reactor; Pareto plot.

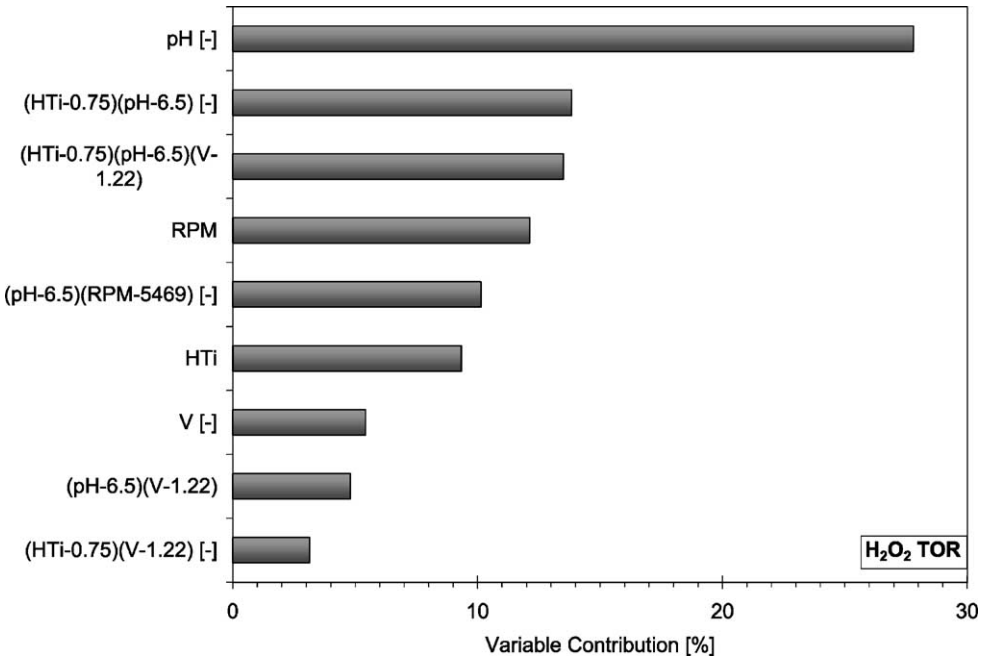

Fig. 10. Effect of reaction variables on the turnover rate (TOR) of H_2O_2 molecules measured in (mol H_2O_2/mol Ti/min) units; Pareto plot.

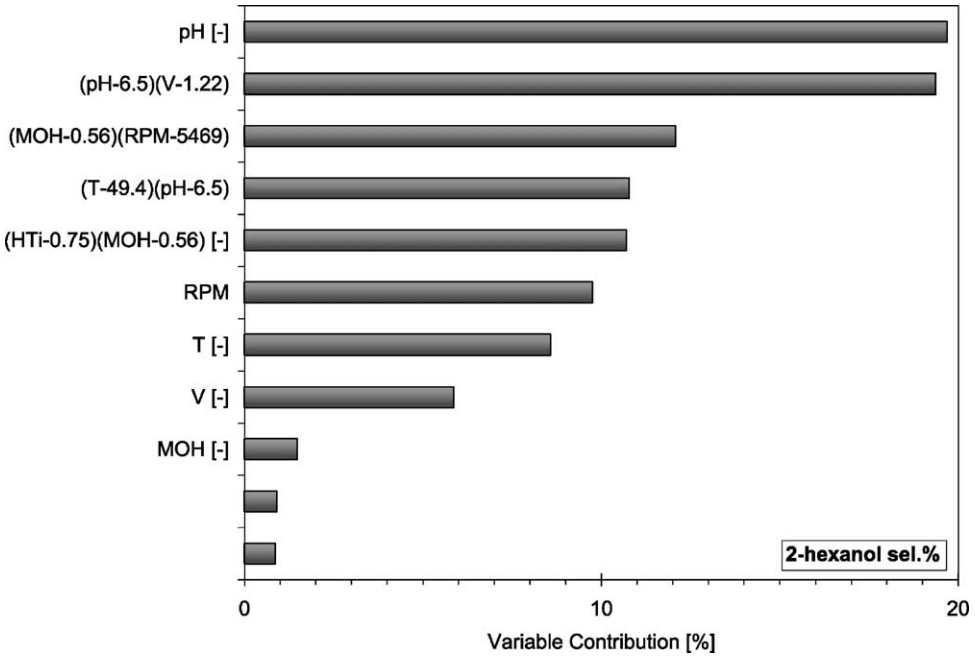

Fig. 11. Effect of reaction variables on the selectivity for 2-hexanol in the oxyfunctionalization of *n*-hexane by 30% aqueous H_2O_2 over TS-PQ^{TM} catalyst; Pareto plot.

effect of other variables also seems to be important (Figs. 11 and 12). Lower temperature can improve the selectivity for 2-hexanol while lower catalyst loading (HTi) can result in higher 3-hexanol yield. Figs. 13 and 14 indicate that acidic pH and elevated temperature are needed to produce more 2-hexanone, and low catalyst loading and high temperature are advantageous for the formation of 3-hexanone. Thus, Figs. 11–14 combined suggest that there is a low chance to obtain these oxygenates individually at any combination of reaction variables.

One can also consider the alcohol/ketone ratio as a selectivity aspect. Fig. 15 indicates that lowering the temperature and increasing the stirring rate and H_2O_2 dosing can improve the ratio of 2-hexanol over 2-hexanone. According to Fig. 16, mainly low pH, high stirring rate, and, to a lesser extent, elevated temperature and low methanol content are favorable for improving the 3-hexanol/3-hexanone ratio.

Finally Figs. 17 and 18 show which reaction variables have significant impact on the regioselectivity of the hexane oxygenates, i.e. whether oxyfunctionalization takes place on the second or the third carbon atom of the hexane chain. To date, only enzymes are known to be able to selectively attack the least reactive primary carbon atoms of paraffins [67,68]. The reactivities of the second and third C–H bonds of *n*-hexane are considered to be largely equivalent with each other and, from thermodynamic point of view, the ratio of C2/C3 oxygenates should be close to 1. That reportedly happens over the isomorphously substituted defect free TS-1 catalysts [9,10,13,16,18,22,23,27,28,31]. In contrast, one can calculate that that the ratio of 2-hexanol/3-hexanol stretches from about 0.08 (Experiment # 15 in Table 2) to 0.89 (Experiment # 5 in Table 2) over TS-PQ^{TM} catalyst, i.e. the oxidation preferably occurs in the γ-position over this catalyst. The β-oxidation increases at more acidic pH, but the combined effect of many other variables seems also to be important (Fig. 17). The ratio of 2-hexanone/3-hexanone varies from around 2 (Experiment # 9 in Table 2) to infinity in experiments where 3-hexanone appears. According to Fig. 18 the fraction of 2-hexanone increases in a more acidic environment in the absence of methanol. The increasing 2-hexanone formation is

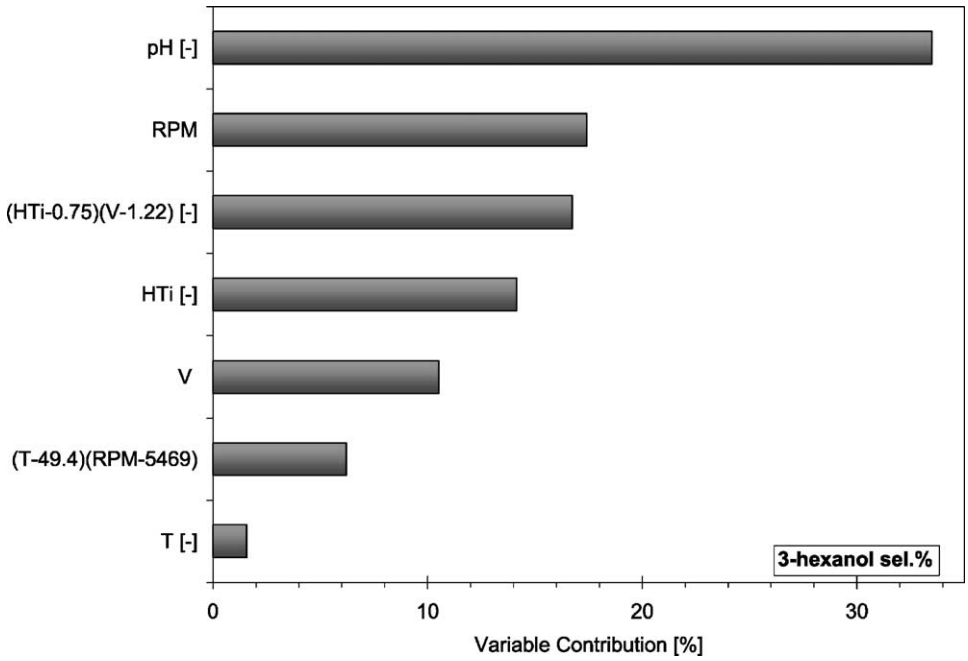

Fig. 12. Effect of reaction variables on the selectivity for 3-hexanol in the oxyfunctionalization of *n*-hexane by 30% aqueous H_2O_2 over TS-PQ^{TM} catalyst; Pareto plot.

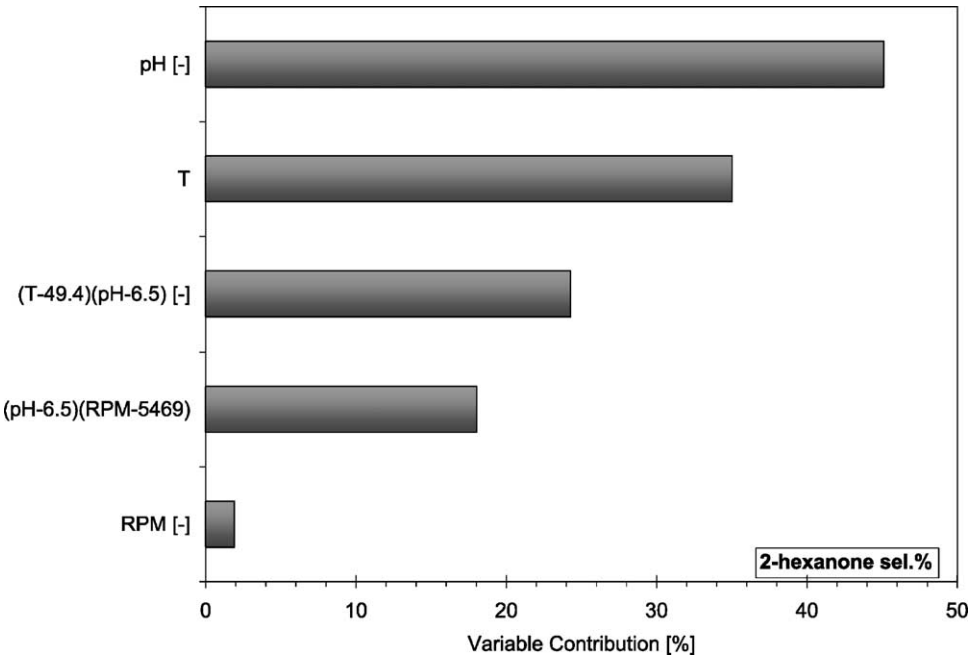

Fig. 13. Effect of reaction variables on the selectivity for 2-hexanone in the oxyfunctionalization of *n*-hexane by 30% aqueous H_2O_2 over TS-PQ^{TM} catalyst; Pareto plot.

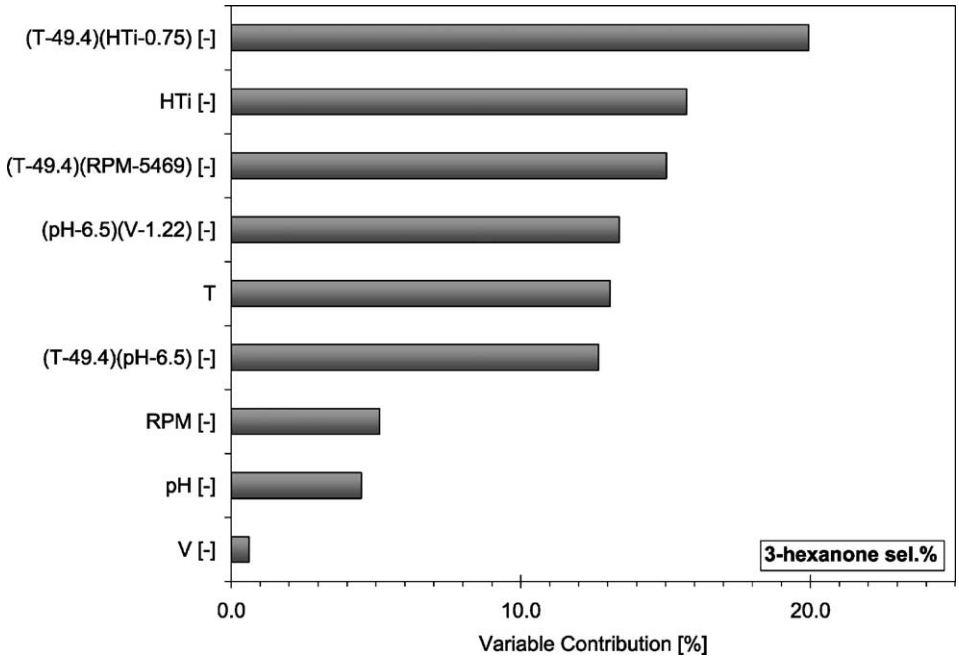

Fig. 14. Effect of reaction variables on the selectivity for 3-hexanone in the oxyfunctionalization of *n*-hexane by 30% aqueous H_2O_2 over TS-PQ^{TM} catalyst; Pareto plot.

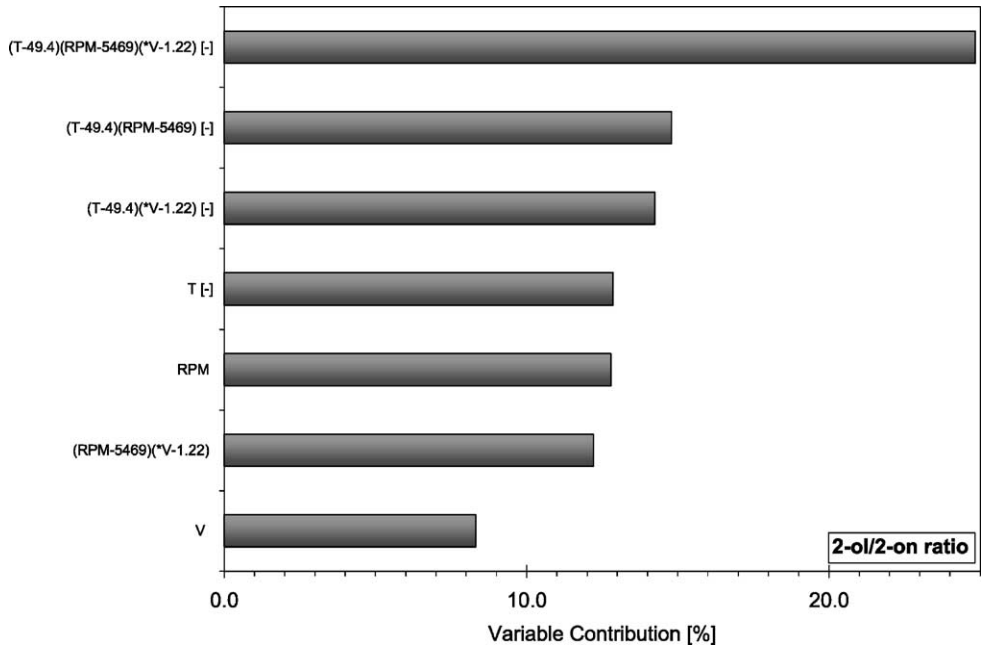

Fig. 15. Effect of reaction variables on the 2-hexanol/2-hexanone ratio in the oxyfunctionalization of *n*-hexane by 30% aqueous H_2O_2 over TS-PQ^{TM} catalyst; Pareto plot.

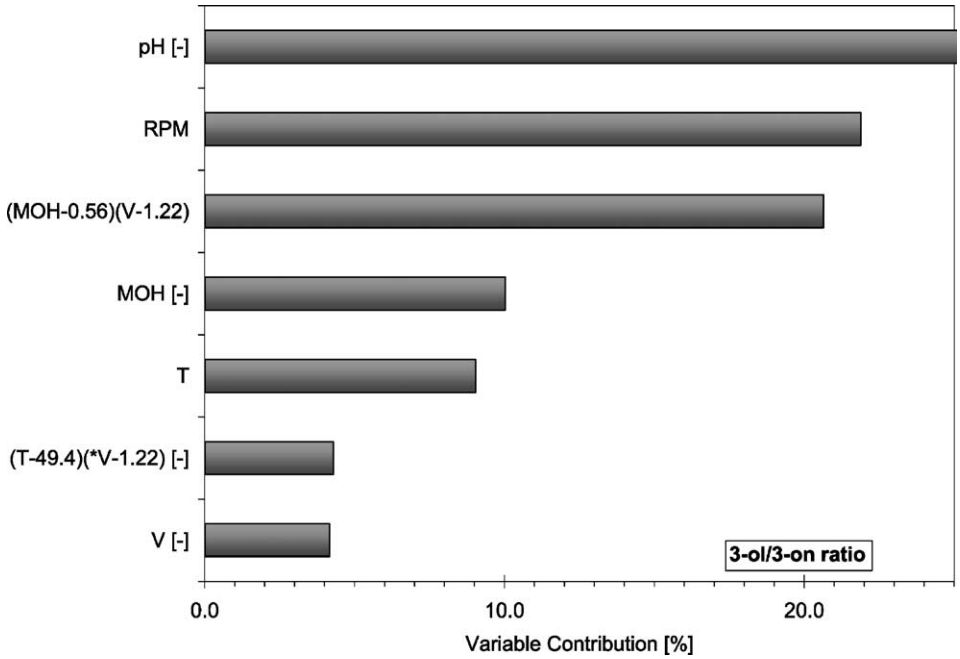

Fig. 16. Effect of reaction variables on the 3-hexanol/3-hexanone ratio in the oxyfunctionalization of *n*-hexane by 30% aqueous H_2O_2 over TS-PQ^{TM} catalyst; Pareto plot.

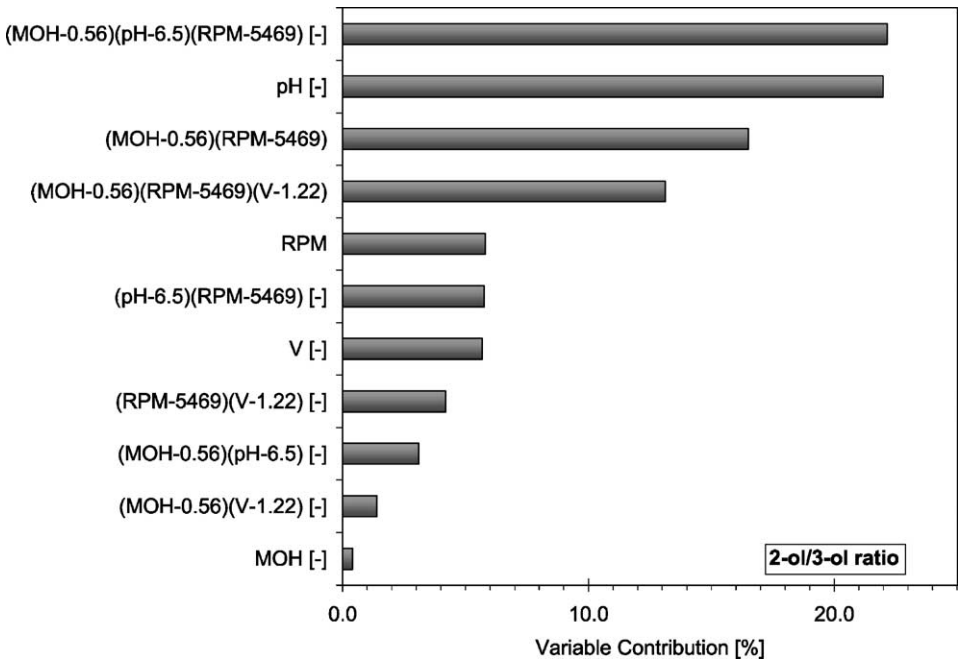

Fig. 17. Effect of reaction variables on the 2-hexanol/3-hexanol ratio in the oxyfunctionalization of *n*-hexane by 30% aqueous H_2O_2 over TS-PQ^{TM} catalyst; Pareto plot.

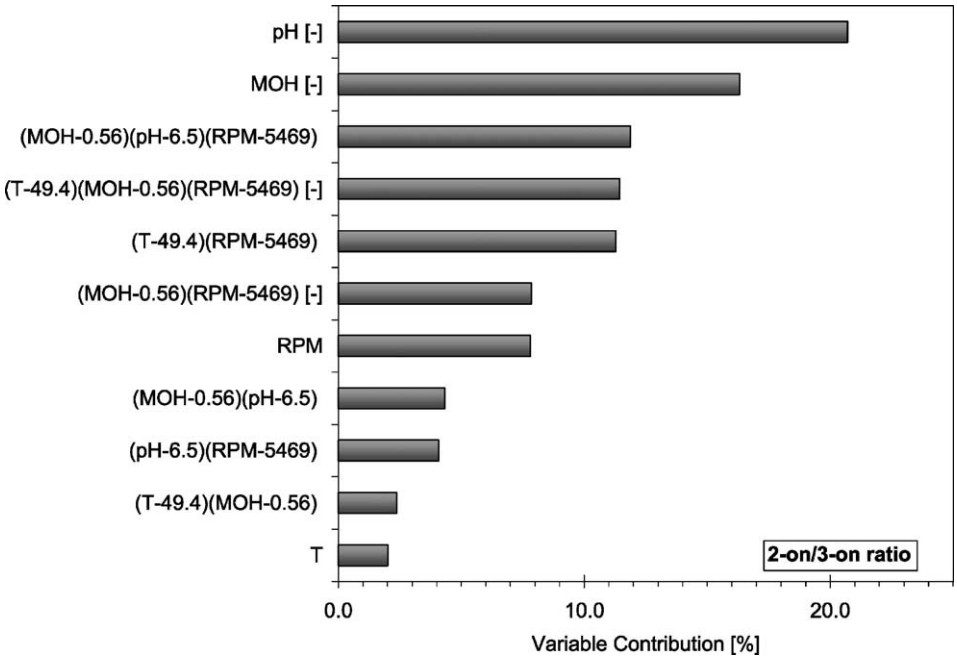

Fig. 18. Effect of reaction variables on the 2-hexanone/3-hexanone ratio in the oxyfunctionalization of *n*-hexane by 30% aqueous H_2O_2 over TS-PQ^{TM} catalyst; Pareto plot.

likely associated with the increasing 2-hexanol production.

4. Discussion

Results in Table 2 and Figs. 6–18 demonstrate that the selection of reaction variables was broad enough to get statistically different reaction rates ranging from zero to outstanding and product compositions that permit selectivity correlations at $r^2 > 0.9$.

Experiment # 5 from Tables 1 and 2 resulted in the highest TOR for *n*-hexane with superior H_2O_2 efficiency (Fig. 2). It is likely that this high H_2O_2 efficiency is an intrinsic catalyst property because it does not correlate with the major reaction variables but depends on the architecture of the active sites within the pentasil titanium silicate structure [34]. The ~200 ppm anatase content in this catalyst could be detected by both laser Raman spectroscopy and by powder XRD; however, it is either inaccessible to the H_2O_2 molecules or has negligible catalytic activity for the decomposition of peroxide. It appears that those catalytic sites that are effective in the oxyfunctionalization of paraffins are not effective for the decomposition of H_2O_2.

The FT-UV spectra of TS-PQ^{TM} silicate in Fig. 3 shows little absorption at <210 nm, correlating to isomorphously substituted, isolated, tetrahedral Ti^{4+} ions in a largely defect free MFI type crystal lattice [4,34,36,51–56]. However, large bands appear in the 220–320 nm range that are characteristic for various non-isolated tetrahedral and octahedral titanium ions. In contrast to a typical TS-1 [3], these absorption bands get even more apparent upon dehydrating the TS-PQ^{TM} silicate at 400 °C and 10^{-3} Pa. The strong 960 cm^{-1} IR bands in Fig. 5 indicates that most Ti^{4+} ions are chemically bonded to the silica lattice of TS-PQ^{TM} catalyst. An improbably high, 3–1500 s. virtual residence time range (Table 2) and the negligible effect of temperature and stirring rate on the TOR of *n*-hexane (Fig. 8) that would affect diffusion suggest that probably only a fraction of Ti^{4+} ions participates in the catalytically active site ensembles. The broad hydroxyl vibration band between 3280 and 3650 cm^{-1} in Fig. 4 points toward the presence

of copious lattice defects in the TS-PQ^{TM} silicate structure. It has been conjectured, that the presence of extralattice Ti^{4+} ions and various lattice defects are advantageous for the catalytic activity of microporous titanium silicates [34,37–41,45,46], yet we are not sure which structural features contribute to the excellent catalytic activity and H_2O_2 efficiency of TS-PQ^{TM} silicate.

Examples in Fig. 1 and Table 2 demonstrate that the oxidation of *n*-hexane levels off after reaching a certain conversion at a given set of reaction parameters despite the presence of ample unreacted *n*-hexane and H_2O_2. It has been shown before that this phenomenon is repeatable within a few percent error [34]. However, we could not find a way to overcome this premature catalyst deactivation. Figs. 6–18 indicate that using methanol cannot help because this co-solvent has either negligible or even retarding effect on most activity and selectivity parameters studied.

Except for the ratio of co-solvent, every variable that was taken into account in Table 1 had statistically significant impact on more than one activity or selectivity parameter of the catalytic reaction. The effect of pH is the most striking. The acidity seems to be advantageous for almost every aspect of the oxyfunctionalization of *n*-hexane by aqueous H_2O_2 over TS-PQ^{TM} catalyst except for the reaction time (Fig. 7), the selectivity for 3-hexanone (Fig. 14), and the ratio of 2-hexanol/2-hexanone (Fig. 15). Oxidation of paraffins in acidic medium by H_2O_2 or a mixture of $O_2 + H_2$ has been also reported over TS-1 [10,21,26]. However the role of acidity is not clear. Except in the presence of superacids [69], the oxidation of saturated hydrocarbons typically proceeds via a radical pathway [70–75]. Various radical mechanisms have also been proposed for the oxyfunctionalization of paraffins over TS-1 [10,16,24,27,33]. Although H-ZSM5 and other Brönsted acid zeolites can promote the oxidation of hydrocarbons and other organic molecules at certain conditions [76–81], the Brönsted acidity of TS-1 type titanosilicates, if any, is very weak [3,10,34] and considered to be either neutral [9] or detrimental [36] for the oxyfunctionalization of hydrocarbons by aqueous H_2O_2. Notwithstanding, one can speculate that the added mineral acids might form temporary, strong, catalytically active Brönsted acid sites on the catalyst surface. Other possible roles for the protons in the liquid phase could be in promoting the generation of $HO–OH_2^+$ intermediates or $OH^\bullet$ radicals required to initiate the catalytic oxidation process, or by forming $\equiv Si–OH_2^+$, $HO_2^\bullet$ or other chain terminating intermediates to prevent a loss in selectivity caused by chain propagation [19,33,50,70,76,78].

In summary, data demonstrate that the TS-PQ^{TM} silicate is an excellent catalyst for the oxyfunctionalization of *n*-hexane by aqueous H_2O_2 especially at slightly acidic conditions in the absence of a co-solvent. The pH, stirring rate, catalyst loading, and other reaction variables affect the rate, the selectivity, and the duration of this reaction. Thus, parameter optimization can be made for one or another of these aspects but not for all at the same time. Details of structure and catalytically active sites of this microporous titanium silicate along with the reaction mechanism have yet to be explored. For a true kinetic analysis it is also desirable to separate the effect of reaction variables on transport phenomena and surface processes.

Acknowledgements

The authors thank Jeff Fuess, Zeolyst International, for his help in navigating in the JMP software and Larry Meyer, SAS Institute, for guidance in experimental design and data analysis related statistics.

References

[1] T. Tatsumi, M. Nakamura, S. Negishi, H. Tominaga, J. Chem. Soc., Chem. Commun. 476 (1990).
[2] D.R.C. Huybrechts, L. De Bruycker, P.A. Jacobs, Nature 345 (1990) 240.
[3] B. Notari, Adv. Catal. 41 (1996) 253.
[4] G. Perego, R. Millini, G. Bellussi, in: Molecular Sieves, Springer, Berlin, 1998, p. 188.
[5] R.J. Saxton, Top. Catal. 9 (1999) 43.
[6] X. Yang, J.-L. Paillaud, H.F.W.J. van Breukelen, H. Kessler, E. Duprey, Microporous Macroporous Mater. 46 (2001) 1.
[7] P. Wu, T. Tatsumi, T. Komatsu, T. Yashima, J. Phys. Chem. B 105 (2001) 2897.
[8] I.W.C.E. Arends, R.A. Sheldon, Appl. Catal. A Gen. 212 (2001) 175.
[9] D.R.C. Huybrechts, I. Vaesen, H.X. Li, P.A. Jacobs, Catal. Lett. 8 (1991) 237.
[10] M. Clerici, Appl. Catal. 68 (1991) 249.
[11] J.S. Reddy, S. Sivasanker, Catal. Lett. 11 (1991) 241.
[12] T. Tatsumi, K. Yuasa, H. Tominaga, J. Chem. Soc., Chem. Commun. 1446 (1992).

[13] M.G. Clerici, B. Anfossi, G. Bellussi, US Patent 5,126,491 (1992).
[14] M.G. Clerici, P. Ingallina, R. Millini, in: Proceedings of the Nineth International Zeolite Conference, Montreal, Canada, 1992, p. 445.
[15] A. Esposito, F. Maspero, U. Romano, in: Proceedings of the DGMK Conference on Selective Oxidations in Petrochemistry, Goslar, Germany, 1992, p. 195.
[16] D.R.C. Huybrechts, P.L. Buskens, P.A. Jacobs, J. Mol. Catal. 71 (1992) 129.
[17] C. Ferrini, H.W. Kouwenhoven, in: Proceedings of the DGMK Conference on Selective Oxidations in Petrochemistry, Goslar, Germany, 1992, p. 205.
[18] P.J. Kooyman, J.C. Jansen, H. van Bekkum, in: Proceedings of the Nineth International Zeolite Conference, Montreal, Canada, 1992, p. 505.
[19] C.B. Khouw, H.X. Li, M.E. Davis, in: Proceedings of the Symposium on Catalytic Selective Oxidation, Presented Before the Division of Petroleum Chemistry, Inc., ACS, Washington, DC, USA, 1992, p. 1136.
[20] C.B. Khouw, C.B. Dartt, H.X. Li, M.E. Davis, in: Proceedings of the 206th National Symposium on New Catalytic Chemistry Utilizing Molecular Sieves, Presented Before the Division of Petroleum Chemistry, Inc., ACS, Chicago, USA, 1993, p. 769.
[21] M.G. Clerici, G. Bellussi, US Patent 5,235,111 (1993).
[22] T. Tatsumi, K. Asano, K. Yanagisawa, Stud. Surf. Sci. Catal. 84 (1994) 1861.
[23] H. Fu, S. Kaliaguine, J. Catal. 148 (1994) 540.
[24] C.B. Khouw, C.B. Dartt, J.A. Labinger, M.E. Davis, J. Catal. 149 (1994) 195.
[25] J.S. Reddy, R. Kumar, S.M. Csicsery, J. Catal. 145 (1994) 73.
[26] M.G. Clerici, B. Anfossi, G. Bellussi, US Patent 5,409,876 (1995).
[27] I.W.C.E. Arends, R.A. Sheldon, M. Wallau, U. Schuchardt, Angew. Chem. Int. Ed. Engl. 36 (1997) 1144.
[28] P. Fejes, A. Horvath, J. Halasz, J.B. Nagy, K. Lazar, Magy. Kem. Foly. 103 (1997) 531.
[29] N. Jappar, Q. Xia, T. Tatsumi, J. Catal. 180 (1998) 132.
[30] S.Q. Wu, C. Bouchard, S. Kaliaguine, in: Proceedings of the 12th International Zeolite Conference, Baltimore, USA, 1999, p. 1399.
[31] G. Langhendries, D.E. De Vos, G.V. Baron, P.A. Jacobs, J. Catal. 187 (1999) 453.
[32] T. Tatsumi, K.A. Koyano, Y. Shimizu, Appl. Catal. A Gen. 200 (2000) 125.
[33] M.G. Clerici, Top. Catal. 15 (2001) 257.
[34] I. Halasz, M. Agarwal, E. Senderov, B. Marcus, Appl. Catal. A Gen. 241 (2003) 167.
[35] G. Geobaldo, S. Bordiga, A. Zecchina, E. Giamello, G. Leofanti, G. Petrini, Catal. Lett. 16 (1992) 109.
[36] G.N. Vayssilov, Catal. Rev. Sci. Eng. 39 (1997) 209.
[37] A. Tuel, Y. Ben Taarit, Appl. Catal. A Gen. 110 (1994) 137.
[38] C. Lamberti, S. Bordiga, D. Arduino, A. Zecchina, F. Geobaldo, G. Spano, F. Genoni, G. Petrini, A. Carati, F. Villain, G. Vlaic, J. Phys. Chem. B 102 (1998) 6382.
[39] J.F. Bengoa, N.G. Gallegos, S.G. Marchetti, A.M. Alvarez, M.V. Cagnoli, A.A. Yeramian, Microporous Macroporous Mater. 24 (1998) 163.
[40] P. Fejes, J.B. Nagy, J. Halasz, A. Oszko, Appl. Catal. A Gen. 175 (1998) 89.
[41] P. Fejes, J.B. Nagy, K. Lazar, J. Halasz, Appl. Catal. A Gen. 190 (2000) 117.
[42] J. Halasz, A. Ell, D. Mehn, E. Meretei, I. Kiricsi, React. Kinet. Catal. Lett. 74 (2001) 371.
[43] N.G. Gallegos, A.M. Alvarez, J.F. Bengoa, M.V. Cagnoli, S.G. Marchetti, A.A. Yeramian, Stud. Surf. Sci. Catal. 135 (2001) P14.
[44] C. Lamberti, S. Bordiga, A. Zecchina, G. Artioli, G. Marra, G. Spano, J. Am. Chem. Soc. 123 (2001) 2204.
[45] G. Li, X. Wang, X. Guo, S. Liu, Q. Zhao, X. Bao, L. Lin, Mater. Chem. Phys. 71 (2001) 195.
[46] G. Bellussi, A. Carati, M.G. Clerici, G. Maddinelli, R. Millini, J. Catal. 133 (1992) 220.
[47] E. Senderov, R. Hinchey, I. Halasz, US Patent, application pending.
[48] JMP Statistical Discovery Software, SAS Institute Inc., 2000. see also http://www.JMPdiscovery.com.
[49] CRC Handbook of Chemistry and Physics, 77th ed., CRC Press, Boca Raton, London, 1996.
[50] A.F. Holleman, E. Wiberg, Inorganic Chemistry, Academic Press, Berlin, 2001.
[51] E. Astorino, J.B. Peri, R.J. Willey, G. Busca, J. Catal. 157 (1995) 482.
[52] A. Zecchina, S. Bordiga, C. Lamberti, G. Ricchiardi, C. Lamberti, G. Ricchiardi, D. Scarano, G. Petrini, G. Leofanti, M. Mantegazza, Catal. Today 32 (1996) 97.
[53] R.C. Drago, S.C. Dias, J.M. McGilvray, A.L.M. Mateus, J. Phys. Chem. B 102 (1998) 1508.
[54] A. de Lucas, L. Rodriguez, P. Sanchez, Appl. Catal. A Gen. 180 (1999) 375.
[55] N. Ulagappan, H. Frei, J. Phys. Chem. 104 (2000) 7834.
[56] T. Armaroli, F. Milella, B. Notari, R.J. Willey, G. Busca, Top. Catal. 15 (2001) 63.
[57] S. Klein, B.M. Weckhuysen, J.A. Martens, W.F. Maier, P.A. Jacobs, J. Catal. 163 (1996) 489.
[58] X. Gao, I.E. Wachs, Catal. Today 51 (1999) 233.
[59] C. Lamberti, Microporous Macroporous Mater. 30 (1999) 155.
[60] X.-S. Wang, X.-W. Guo, Catal. Today 51 (1999) 177.
[61] P. Wu, T. Tatsumi, T. Komatsu, T. Yashima, J. Phys. Chem. B 105 (2001) 2897.
[62] A. Zecchina, S. Bordiga, G. Spoto, L. Marchese, G. Petrini, G. Leofanti, M. Padovan, J. Phys. Chem. 96 (1992) 4991.
[63] G. Ricchiardi, A. Damin, S. Bordiga, C. Lamberti, G. Spano, F. Rivetti, A. Zecchina, J. Am. Chem. Soc. 123 (2001) 11409.
[64] I. Halasz, S. Kim, B. Marcus, Molecular Physics, 100 (2002) 3123.
[65] G.A. Somorjai, The Building of Catalysts in Catalyst Design, in: L.L. Hegedus et al. (Eds.), Wiley, 1987.
[66] G. Ertl, Dynamics of Reactions at Surfaces in Impact of Surface Science on Catalysis, B.C. Gates, H. Knözinger (Eds.), Academic Press, London, 2000.
[67] K.S. Suslick, in: C.L. Hill (Ed.), Activation and Functionalization of Alkanes, Wiley, New York, 1989, p. 219.

[68] C.A. Tolman, J.D. Druliner, M.J. Nappa, N. Herron, in: C.L. Hill (Ed.), Activation and Functionalization of Alkanes, Wiley, New York, 1989, p. 303.
[69] G.A. Olah, O. Farooq, G.K.S. Prakash, in: C.L. Hill (Ed.), Activation and Functionalization of Alkanes, Wiley, New York, 1989, p. 27.
[70] S.W. Benson, Prog. Energy Combust. Sci. 7 (1981) 125.
[71] K.S. Suslick, in: C.L. Hill (Ed.), Activation and Functionalization of Alkanes, Wiley, New York, 1989, p. 219.
[72] C.A. Tolman, J.D. Druliner, M.J. Nappa, N. Herron, in: C.L. Hill (Ed.), Activation and Functionalization of Alkanes, Wiley, New York, 1989, p. 303.
[73] A.E. Shilov, A.A. Shteinman, Acc. Chem. Res. 32 (1999) 763.
[74] M.Yu. Sinev, L.Ya. Margolis, V.N. Korchak, Russ. Chem. Rev. 64 (1995) 349.
[75] M. Xu, T.H. Ballinger, J.H. Lunsford, J. Phys. Chem. 99 (1995) 14494.
[76] I. Halasz, A. Brenner, M. Shelef, K.Y.S. Ng, J. Phys. Chem. 99 (1995) 17186.
[77] I. Halasz, A. Brenner, K.Y.S. Ng, Catal. Lett. 34 (1995) 151.
[78] I. Halasz, A. Brenner, K.Y.S. Ng, Y. Hou, J. Catal. 161 (1996) 359.
[79] I. Halasz, A. Brenner, Catal. Lett. 51 (1998) 195.
[80] C.D. Chang, S.D. Hellring, US Patent 4,578,521 (1986).
[81] D.R.C. Huybrechts, R.F. Parton, P.A. Jacobs, Stud. Surf. Sci. Catal. 60 (1991) 225.